Axial Strain Sensor Based on Microfiber Couplers Operating at the Dispersion Turning Point

Jiajie Wen, Xiangyu Yan, Xu Gao, Kaiwei Li, *Member, IEEE*, and Jiajia Wang

***Abstract*—A novel axial strain sensor based on an optical microfiber coupler (OMC) operating at the dispersion turning point (DTP) was designed to realize high-sensitivity measurements of axial strain. First, we explain the measurement principle of axial strain sensors based on microfiber couplers. Then, we calculate the measurements, with the theoretical calculations showing that the sensor has high sensitivity when the effective refractive index (ERI) difference between the odd and even modes in the coupling region of the OMC is equal to zero. Finally, we carried out axial tensile experiments on the OMC. The results show that the OMC has the highest axial strain sensitivity when it operates at the DTP. The maximum sensitivity is 166.9 pm/$\mu\varepsilon$, with a linear range of 0-400 $\mu\varepsilon$. The sensor is highly sensitive to axial strains and has a simple structure. It has broad application prospects in the measurement of mechanical quantities such as strain, acceleration and vibration.**

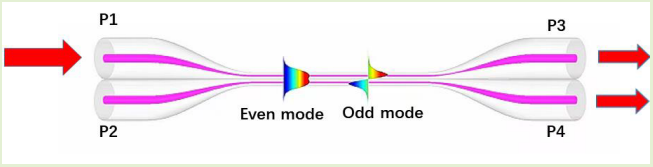

***Index Terms*—Optical microfiber coupler, dispersion turning point, axial strain sensing, spectral drift.**

I. Introduction

In RECENT years, optical fiber sensing has been widely used in humidity, temperature, refractive index, biological monitoring, strain measurement and so on [1]–[4]. For strain measurement, researchers have proposed many strain sensing technologies based on optical fiber sensing. Optical fiber strain sensors are compact structures with strong anti-electromagnetic interference abilities, high sensitivity, and low cost. Currently, these sensors have been widely used in engineering fields such as bridge monitoring, aircraft wing bending monitoring and mechanical equipment monitoring. In 2013, Zheng J *et al.* proposed a strain sensor based on a Mach Zehnder interferometer with a strain sensitivity of 2.1 pm/$\mu\varepsilon$ [5]. In 2014, Chuanxu Liu *et al.* proposed a tapered thin-core fiber strain sensor fabricated by arc-discharged splicing and taper techniques with a strain sensitivity of 0.119 dB/$\mu\varepsilon$ [6]. In 2020, Gao *et al.* proposed a few-mode fiber and FBG with a strain sensitivity of 2 pm/$\mu\varepsilon$ [7]. However, some of the strain sensors described above have low sensitivity and cannot measure large strains. In addition, sensor structures based on Fabry-Perot interferometers or FBG grating technology are more complex, and the demodulation equipment requirements are relatively high [8]–[12]. Therefore, the development of a new optical fiber strain sensor with a simple structure, high sensitivity, and low demodulation equipment requirements has attracted the attention of researchers.

According to previous research, the optical fiber coupler excites the odd and even modes at a specific input light wavelength and a specific coupling region diameter. When the group ERIs of the odd mode and even mode are equal, the corresponding wavelength is called the dispersion turning point (DTP). The DTP characteristics can be used to achieve high-sensitivity measurements of refractive indices (RI) or strain. For example, in 2016, Kaiwei Li *et al.* proposed an RI sensor based on an OMC that used the DTP of the optical fiber odd and even mode group effective refractive indices (ERIs) to achieve an ultrahigh RI sensitivity of

Manuscript received January 10, 2022; accepted January 12, 2022. Date of publication January 14, 2022; date of current version February 28, 2022. This work was supported in part by the State Key Laboratory of Applied Optics under Grant SKLAO2021001A03, in part by the Key Research and Development of Jilin Provincial Department of Science and Technology-Key Industrial Core Technology Research Project (20210201091GX), and in part by the National Natural Science Foundation of China under Grant 62005101. The associate editor coordinating the review of this article and approving it for publication was Prof. Carlos Marques. *(Jiajie Wen and Xiangyu Yan contributed equally to this work.) (Corresponding author: Xu Gao.)*

Jiajie Wen is with the School of Photoelectric Engineering, Changchun University of Science and Technology, Changchun 130022, China
(e-mail: wenjiajie9504@163.com).

Xiangyu Yan is with the Institute of Photonics Technology, Jinan University, Guangzhou 510632, China (e-mail: 1207231027@qq.com).

Xu Gao is with the State Key Laboratory of Applied Optics and the School of Photoelectric Engineering, Changchun University of Science and Technology, Changchun 130022, China (e-mail: gaox19870513@163.com).

Kaiwei Li is with the Key Laboratory of Bionic Engineering, Ministry of Education, Jilin University, Changchun 130022, China (e-mail: kaiwei_li@jlu.edu.cn).

Jiajia Wang is with the College of Agricultural Equipment Engineering, Henan University of Science and Technology, Luoyang 471003, China (e-mail: jjw@haust.edu.cn).

Digital Object Identifier 10.1109/JSEN.2022.3143696

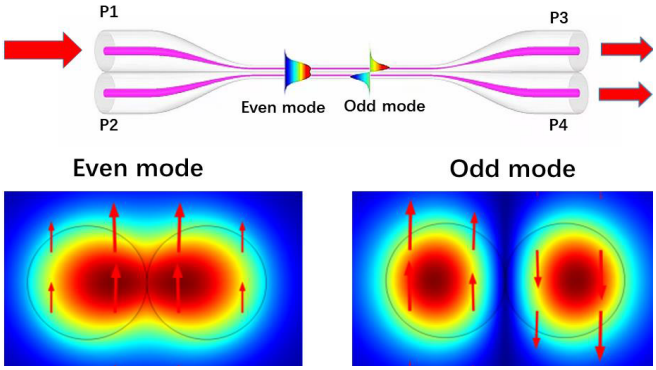

Fig. 1. Schematic diagram of the OMC and the odd and even mode modular field distributions.

39541.7 nm/RIU. Compared with traditional fiber couplers, the RI measurement sensitivity can be two orders of magnitude higher when the sensor operates at the DTP [13]. In 2021, Kaijun Liu *et al.* proposed a strain sensor based on the DTP and a Mach– Zehnder interferometer, with a strain sensitivity of -45.55 pm/$\mu\varepsilon$ [14]. The application of the DTP provides a new high-sensitivity measurement method for use in chemistry, biology, and other fields.

The OMC is made of two optical fibers that are tapered by electric discharge or flame heating. Because the spectral ratio is easily changed by external interference, it has attracted extensive attention from researchers in recent years. We designed and manufactured an OMC operating at the DTP with a coupling length diameter of approximately 2.53 μm and a coupling length of 40 mm that achieved an axial strain sensitivity of 166.9 pm/$\mu\varepsilon$ and a linear range of 0-400 $\mu\varepsilon$. The sensor has a simple structure, low demodulation equipment requirements, and a low cost, providing a new method for axial strain detection.

II. Principle Analysis and Simulation Calculation

A. Principle of the OMC

We use software COMSOL Multiphysics 5.5 to analyze the ERI changes of the odd and even modes of the OMC during stretching to simulate the effect of axial stretching on the OMC transmission power. As shown in Fig. 1, the OMC is formed by fusion splicing two single-mode fibers and includes a coupling area, two input ports and two output ports. In the coupler, the coupling area of the two microfibers forms a new waveguide. When light enters the conical transition region from port 1, it can simultaneously excite the even and odd modes. The two modes propagate along the waveguide, and a phase difference gradually accumulates; finally, the two modes couple to the two output ends, which leads to mode interference. Therefore, the energy distributions of the optical paths differ, resulting in different interference stripes at the output ends [15], [16].

P1 is the input optical power, and the output energies of output ports 3 and 4 are:

$$P_3 = P_1 \cos^2\left(\frac{1}{2}\phi\right) \tag{1}$$

$$P_4 = P_1 \sin^2\left(\frac{1}{2}\phi\right) \tag{2}$$

The phase difference ϕ between the two modes satisfies:

$$\phi_N = \frac{2\pi L(n_{\text{eff}}^{\text{even}} - n_{\text{eff}}^{\text{odd}})}{\lambda_N} = (2N-1)\,\pi \tag{3}$$

where n_{eff}^{even} and n_{eff}^{odd} are the effective refractive indices of the odd mode and even mode, respectively; β is the propagation constant of the mode; and L is the coupling length. When the coupling region of the OMC is strained, the ERIs of the odd and even modes change. In this study, we considered only the uniform waist region, as it is much thinner, much longer, and much more sensitive than the tapered region [17]–[20].

Eq. (3) can be expressed as:

$$2\pi L(n_{\text{eff}}^{\text{even}} - n_{\text{eff}}^{\text{odd}}) = (2N-1)\,\pi\,\lambda_N \tag{4}$$

By taking a slight variation from Eq. (4), the spectral dependency on length L is obtained as:

$$\begin{aligned} &2\pi \frac{\partial L}{\partial L}\left(n_{\text{eff}}^{\text{even}} - n_{\text{eff}}^{\text{odd}}\right) \\ &\quad +2\pi L\left(\frac{\partial\left(n_{\text{eff}}^{\text{even}} - n_{\text{eff}}^{\text{odd}}\right)}{\partial L} + \frac{\partial\left(n_{\text{eff}}^{\text{even}} - n_{\text{eff}}^{\text{odd}}\right)}{\partial \lambda_N}\frac{\partial \lambda_N}{\partial L}\right) \\ &\quad = (2N-1)\,\pi \frac{\partial \lambda_N}{\partial L} \end{aligned} \tag{5}$$

Then, Bring Eq. (3) into Eq. (5) and reorganize we can obtain:

$$S_L = \frac{\partial \lambda_N}{\partial L} = \frac{\lambda_N(\Delta n_{\text{eff}}/L + \partial(\Delta n_{\text{eff}})/\partial L)}{n_g^{\text{even}} - n_g^{\text{odd}}} \tag{6}$$

where $\Delta n_{\text{eff}} = n_{\text{eff}}^{\text{even}} - n_{\text{eff}}^{\text{odd}}$, and the group effective refractive index n_g satisfies:

$$n_g^{\text{even}} = n_{\text{eff}}^{\text{even}} - \lambda_N \frac{\partial n_{\text{eff}}^{\text{even}}}{\partial \lambda_N} \tag{7}$$

$$n_g^{\text{odd}} = n_{\text{eff}}^{\text{odd}} - \lambda_N \frac{\partial n_{\text{eff}}^{\text{odd}}}{\partial \lambda_N} \tag{8}$$

The tensile strain of the optical fiber is $\delta = \partial L/L$. Thus, the sensitivity of the corresponding coupler strain can be deduced as:

$$S_\delta = \frac{\partial \lambda_N}{\partial \delta} = \frac{\lambda_N}{n_g^{\text{even}} - n_g^{\text{odd}}}\left(\Delta n_{\text{eff}} + \frac{\partial \Delta n_{\text{eff}}}{\partial \delta}\right) \tag{9}$$

$\partial(\Delta n_{eff})/\partial L)$ mainly depends on the calender coefficient (the change in refractive index caused by stretching) and the change in diameter caused by stretching. It can be seen from the formula that the sensitivity curve of the coupler also has a dispersion inflection point, when $n_g^{even} - n_g^{odd} = 0$, which is the point of maximum sensitivity immediately, and we call it dispersion turning point (DTP).

B. Axial Strain Simulation of the OMC

To prove the theory, we use software COMSOL Multiphysics 5.5 to calculate the effective refractive indices (ERI) of the odd and even modes of the OMC under different diameters and input light wavelengths. As shown in Fig. 2, according to Eq. (7) and (8), we calculated the group ERI differences when the fiber coupler had a diameter of 2.4 μm, 2.6 μm, 2.8 μm, or 3.0 μm. Moreover, as shown in Fig. 3, according

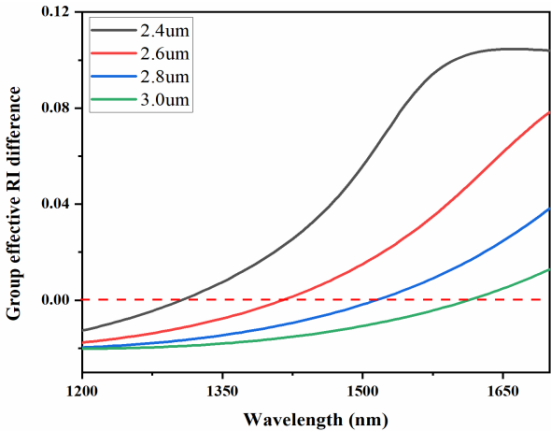

Fig. 2. Group ERI difference between the odd and even mode groups in different diameters.

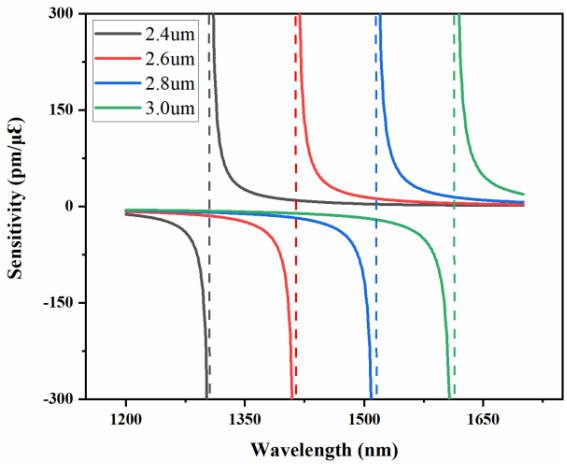

Fig. 3. The axial strain sensitivity of the OMC at diameters of 2.4 μm, 2.6 μm, 2.8 μm, and 3.0 μm.

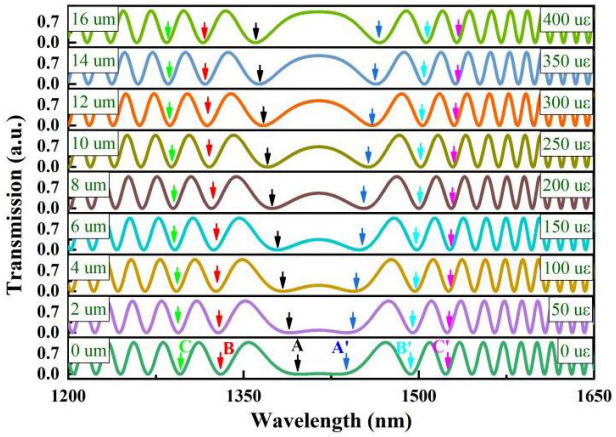

Fig. 4. Spectra of OMC under different strains when the diameter is 2.6 μm and the length is 40 mm.

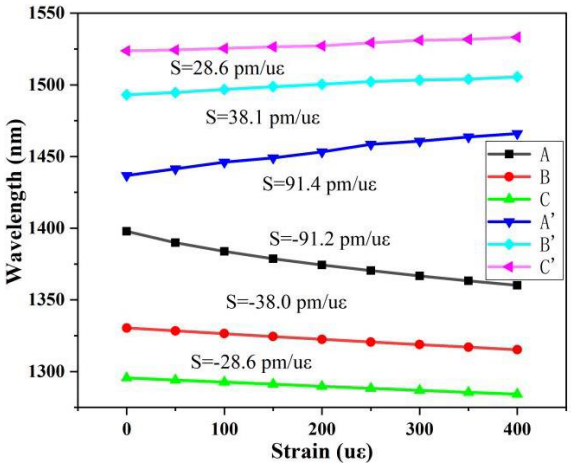

Fig. 5. Axial strain sensitivity of dips A, B, C, A', B', and C'.

to Eq. (9), we can calculate the sensitivity curves of the fiber coupler with diameters of 2.4 μm, 2.6 μm, 2.8 μm, and 3.0 μm. From Fig. 2 and Fig. 3, we can see that as the coupling diameter of the OMC increases, the wavelength corresponding to the chromatic DTP redshifts. In addition, the closer the interference dip to the DTP, the higher the axial strain sensitivity, and the axial strain sensitivity is the largest at the DTP.

Then, we calculated the output spectrum of an OMC with a diameter of 2.6 μm and a length of 40 mm when it was stretched. We increased the length of the coupler by an increment of 2 μm each time, and the corresponding axial strains were 0, 50, 100, 150, 200, 250, 300, 350, 400 $\mu\varepsilon$ (The diameter change of the coupling region caused by the length change of the OMC was very small, and the shift of the OMC spectrum caused by the length change was very weak, so the influence of axial stretching on the DTP was not considered.). The spectra corresponding to different strains output by the OMC were calculated, as shown in Fig. 4. When the diameter was 2.6 μm, the wavelength of the DTP was approximately 1405 nm. As shown in Fig. 5, the calculated axial strain sensitivities of interference dips A, B, C, A', B' and C' were -91.2 pm/$\mu\varepsilon$, -38.0 pm/$\mu\varepsilon$, -28.6 pm/$\mu\varepsilon$, 91.4 pm/$\mu\varepsilon$, 38.1 pm/$\mu\varepsilon$ and 28.6 pm/$\mu\varepsilon$, respectively, and the OMC has linear outputs at axial strains of 0-400 $\mu\varepsilon$. The theoretical calculation shows that the output spectrum of the OMC is symmetrical about the DTP, so the axial stretching sensitivity of the spectra on both sides is the same; axial stretching moves the spectral trough away from the DTP, causing the left spectrum to blueshift and the right spectrum to redshift. The closer the dip is to the DTP, the higher the axial strain sensitivity.

III. Manufacture of Sensor and Analysis of Axial Strain Experiment

A. Manufacture of Optical Microfiber Couplers

The schematic diagram of the optical fiber tapering setup is shown in Fig. 6. First, we stripped the coating from the middle of the two single-mode fibers to obtain two bare fibers with a length of about 10 mm. After that, we fixed one end of the two optical fibers together on the taper machine platform so that the two optical fibers are entangled with each other to form an intersecting whole, and the other end is also fixed on the taper machine platform. Then, we connected one end of the optical fiber to the light source and the other end to the optical spectrum analyzer (OSA). Finally, we used the flame to scan back and forth to heat the bare fibers, and adjust the vertical distance between the flame and the fiber. After the fiber was

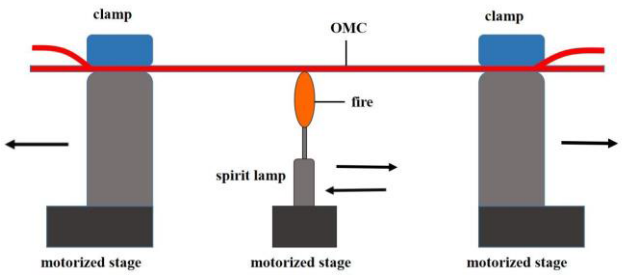

Fig. 6. Schematic of optical fiber coupler tapering device.

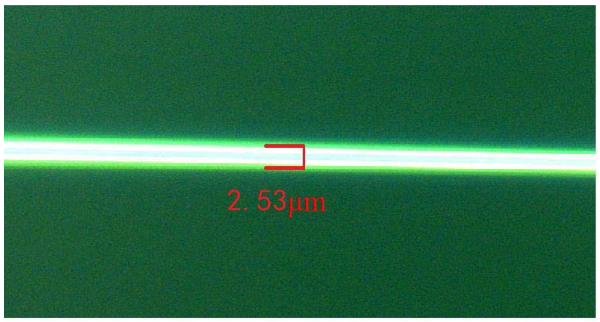

Fig. 7. Microscope image of the OMC coupling region.

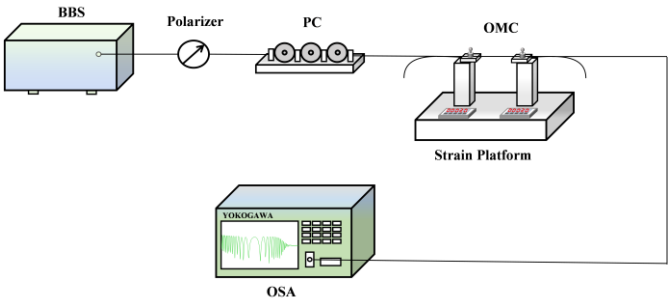

Fig. 8. OMC strain device diagram.

softened, we controlled the tapering machine to draw the fiber to both sides at a constant speed to obtain a microfiber coupler. The diameter of the coupling zone can be precisely adjusted by controlling the taper pulling speed and taper time, and the length of the coupling zone can be controlled by adjusting the flame scanning distance [21]. By observing the output spectrum during the tapering process, the wavelength of the DTP of the fiber coupler can be obtained in real-time. Finally, we fabricated a microfiber coupler with a diameter of 2.53 μm and a coupling length of 40 mm, as shown in Fig. 7.

B. Measuring System

As shown in Fig. 8, the broadband light from the broadband source (BBS) enters the OMC at the input port after passing through the polarizer and polarization controller (PC) and then outputs from the other port, which is directly connected to the OSA (YOKOGAWA AQ6735). First, we fixed the two ends of the OMC to the fiber strain platform; then, we controlled the stretching platform to move by 2 μm; finally, we observed and recorded the output spectrum image of the OMC. The actual strain system is shown in Fig. 9.

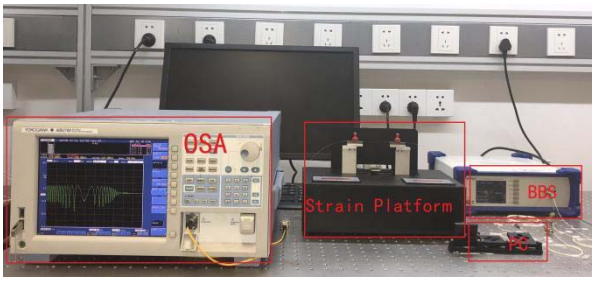

Fig. 9. Actual image of the OMC strain device.

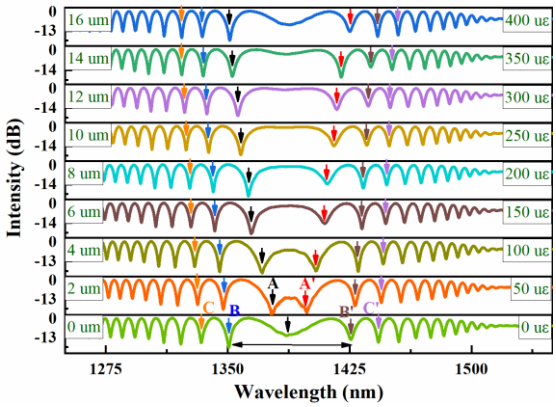

Fig. 10. Spectrum changes with strains of 0-400 $\mu\varepsilon$.

C. Experimental Result

As shown in Fig. 10, the DTP of the OMC was approximately 1390 nm. As the axial strain increases, the spectrum on the left side of the DTP blueshifts, while the spectrum on the right side redshifts. Then, we calculated the axial strain sensitivity by tracing the drifts of the interference dips. As shown in Fig. 11, the axial strain sensitivities of dips A, B, C, A', B', and C' are -83.1 pm/$\mu\varepsilon$, -40.7 pm/$\mu\varepsilon$, -31.2 pm/$\mu\varepsilon$, 83.7 pm/$\mu\varepsilon$, 39.5 pm/$\mu\varepsilon$, and 29.3 pm/$\mu\varepsilon$, respectively, with a linear range of 0-400 $\mu\varepsilon$. The experimental results show that interference dips close to the DTP have improved sensitivities. The symmetrical dip axial strain sensitivity is nearly the same at both ends of the DTP. The final experimental axial sensitivity was essentially equal to the theoretically calculated axial strain sensitivity, proving that an OMC working at the DTP can achieve high-sensitivity axial strain measurements.

Moreover, a sample with a diameter of approximately 2.53 μm and a coupling length of 40 mm was used to perform multiple axial strain experiments. The strain was increased from 0 $\mu\varepsilon$ to 400 $\mu\varepsilon$ and then decreased from 400 $\mu\varepsilon$ to 0 $\mu\varepsilon$. The experiment was repeated several times, and the spectral drift of dip A was recorded. As shown in Fig. 12, as the axial strain increased or decreased, the axial strain sensor based on the OMC showed good repeatability. The average axial sensitivity was calculated to be approximately -82.7 pm/$\mu\varepsilon$, and the maximum deviation was less than 3.4 pm/$\mu\varepsilon$, implying that the repeatability error was less than $\pm 4.1\%$.

We have produced four microfiber couplers with similar coupling zone diameter and coupling length to prove that the microfiber coupler has good reproducibility. The output spectra of the four microfiber couplers at 0 $\mu\varepsilon$ are shown in Fig. 13. Load the four couplers with axial strains of 0-400 $\mu\varepsilon$ and

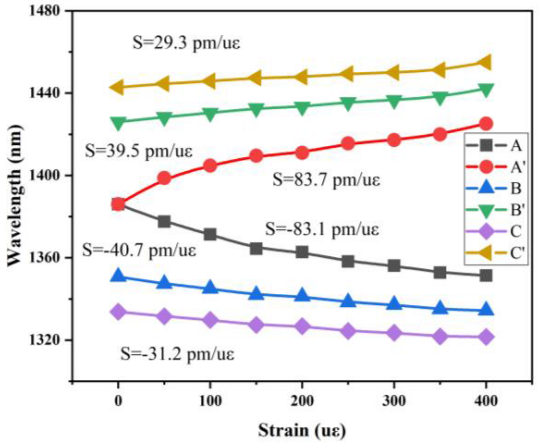

Fig. 11. The axial strain sensitivity of dips A, B, C, A', B', and C'.

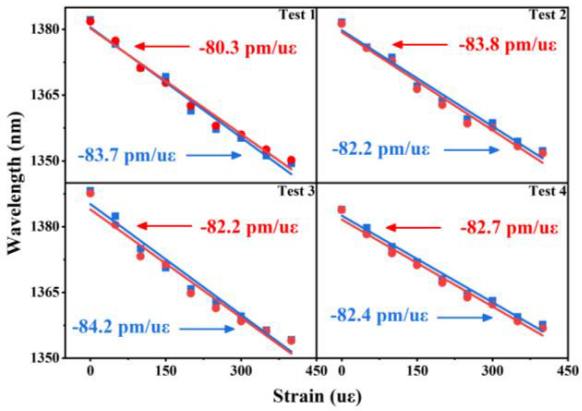

Fig. 12. The relation between the wavelength drift and the increase/decrease in the axial strain.

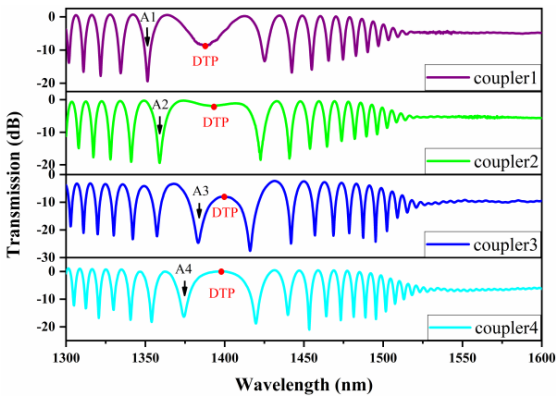

Fig. 13. Output spectra of different couplers at o $\mu\varepsilon$.

record the wavelength change of the first dip on the left of the DTP. Fig. 14 shows the change curve of the valley wavelength of different microfiber couplers with strain. The strain sensitivity of A1, A2, A3, and A4 is -83.1 pm/$\mu\varepsilon$, −86.8 pm/$\mu\varepsilon$, −78.4 pm/$\mu\varepsilon$ and −81.8 pm/$\mu\varepsilon$, and the average sensitivity is −82.3 pm/$\mu\varepsilon$. It can be seen that when the radius of the coupling zone and coupling length are the same, the microfiber coupler has similar DTP and strain sensitivity, and shows good reproducibility.

In addition, the symmetry of the output spectrum with respect to the DTP is a new method for improving measurement sensitivity. As shown in Fig. 15, by analyzing

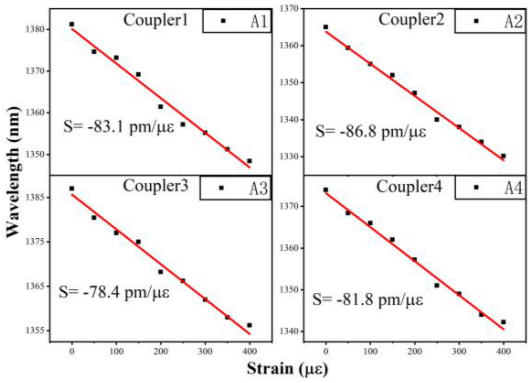

Fig. 14. The axial strain sensitivity of interference dips A1, A2, A3, and A4.

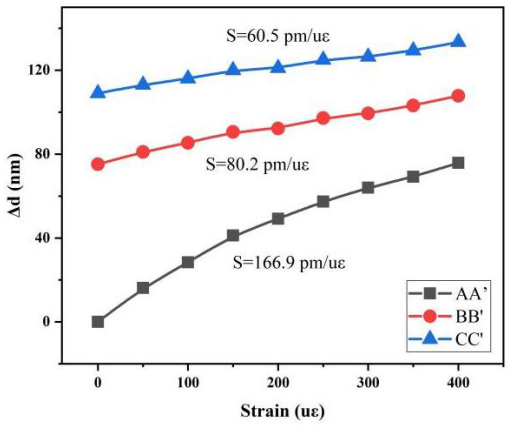

Fig. 15. The axial strain sensitivity of AA', BB', and CC'.

TABLE I
COMPARISON OF FIBER OPTIC STRAIN SENSORS WITH DIFFERENT PRINCIPLES

Structure	Strain sensitivity	Linear Range	Complexity
Mach–Zehnder [5]	2.1 pm/με	0-3000 με	Hight
Tapered Thin-Core Fiber [6]	0.119 dB/με	0-120 με	low
Bubble based micro-cavity [22]	30.66 pm/με	0-600 με	Medium
Few-mode FBG [7]	2 pm/με	0-450 με	low
Mach-Zehnder-DTP [14]	45.55 pm/με	0-600 με	low
FBG and chirp fiber [23]	5.36 pm/με	0-265.49 με	Hight
Few-mode fiber FBG [24]	0.67 pm/με	0-450 με	low
Sagnac-fibre coupling [25]	32 pm/με	0-900 με	Medium
Our work	166.9 pm/με	0-400 με	low

the output spectra of dips AA', BB', CC', we calculated that the axial strain sensitivities of AA', BB' and CC' were 166.9 pm/$\mu\varepsilon$, 80.2 pm/$\mu\varepsilon$ and 60.5 pm/$\mu\varepsilon$, respectively, with

a linear output in the stain range of 0-400 $\mu\varepsilon$. This method of analyzing the interval between the dips on both sides of the DTP nearly doubles the axial strain sensitivity.

Finally, we compare our work with other reported fiber optic strain sensors. As shown in Table I, we compare the sensitivity, linearity and structural complexity of optical fiber axial strain sensors based on different principles. It can be seen that the axial strain sensor based on microfiber couplers working at the DTP has the advantages of higher axial strain sensitivity, simpler structure and larger linear range than other fiber optic strain sensors.

IV. Conclusion

In summary, we propose an axial strain sensor based on a microfiber coupler that operates at the dispersion turning point, and we perform simulation calculations and experimental verifications of the sensor. Both the simulation calculation and the experimental results show that the OMC has higher sensitivity when it operates near the DTP. When the coupling area diameter is 2.53 μm, and the coupling length is 40 mm, the sensor achieves a maximum axial strain sensitivity of 166.9 pm/$\mu\varepsilon$ with a linear output range of 0-400 $\mu\varepsilon$. The sensor has a simple structure and lower requirements for demodulation equipment, and it can achieve high-sensitivity strain measurements. At the same time, it introduces a new idea for measuring physical quantities such as acoustic waves and acceleration, greatly expanding the applications of the microfiber coupler-based device.

References

[1] N. Alberto *et al.*, "Relative humidity sensing using micro-cavities produced by the catastrophic fuse effect," *Opt. Quantum Electron.*, vol. 48, no. 3, p. 216, Mar. 2016.

[2] Y. Mizuno, R. Ishikawa, H. Lee, A. Theodosiou, K. Kalli, and K. Nakamura, "Potential of discriminative sensing of strain and temperature using perfluorinated polymer FBG," *IEEE Sensors J.*, vol. 19, no. 12, pp. 4458–4462, Jun. 2019.

[3] S. Kumar *et al.*, "MoS_2 functionalized multicore fiber probes for selective detection of shigella bacteria based on localized plasmon," *J. Lightw. Technol.*, vol. 39, no. 12, pp. 4069–4081, Jun. 15, 2021.

[4] Z. Wang *et al.*, "Taper-in-taper fiber structure-based LSPR sensor for alanine aminotransferase detection," *Opt. Exp.*, vol. 29, no. 26, pp. 43793–43810, 2021.

[5] J. Zheng *et al.*, "Temperature and index insensitive strain sensor based on a photonic crystal fiber in line Mach–Zehnder interferometer," *Opt. Commun.*, vol. 297, pp. 7–11, Jun. 2013.

[6] C. Liu, D. Sun, J. Yang, H. Zhang, and L. Ran, "Ultra-sensitive intensity modulated strain sensor by tapered thin-core fiber based modal interferometer," *Photonics*, vol. 8, no. 9, p. 372, Sep. 2021.

[7] X. Gao *et al.*, "A dual-parameter fiber sensor based on few-mode fiber and fiber Bragg grating for strain and temperature sensing," *Opt. Commun.*, vol. 454, Jan. 2020, Art. no. 124441.

[8] Z. Gong *et al.*, "High-sensitivity Fabry–Perot interferometric acoustic sensor for low-frequency acoustic pressure detections," *J. Lightw. Technol.*, vol. 35, no. 24, pp. 5276–5279, Dec. 15, 2017.

[9] F. Yu *et al.*, "Ultrasensitive pressure detection of few-layer MoS_2," *Adv. Mater.*, vol. 29, no. 4, Jan. 2017, Art. no. 1603266.

[10] X. Mao *et al.*, "Stabilized fiber-optic Fabry–Perot acoustic sensor based on improved wavelength tuning technique," *J. Lightw. Technol.*, vol. 35, no. 11, pp. 2311–2317, Jun. 1, 2017.

[11] H. Liao *et al.*, "Phase demodulation of short-cavity Fabry–Perot interferometric acoustic sensors with two wavelengths," *IEEE Photon. J.*, vol. 9, no. 2, pp. 1–9, Apr. 2017.

[12] Y. Chen, S.-C. Yan, X. Zheng, F. Xu, and Y.-Q. Lu, "A miniature reflective micro-force sensor based on a microfiber coupler," *Opt. Exp.*, vol. 22, no. 3, p. 2443, Feb. 2014, doi: 10.1364/OE.22.002443.

[13] K. Li, T. Zhang, G. Liu, N. Zhang, M. Zhang, and L. Wei, "Ultrasensitive optical microfiber coupler based sensors operating near the turning point of effective group index difference," *Appl. Phys. Lett.*, vol. 109, no. 10, Sep. 2016, Art. no. 101101.

[14] K. Liu *et al.*, "Highly sensitive vibration sensor based on the dispersion turning point microfiber Mach–Zehnder interferometer," *Opt. Exp.*, vol. 29, no. 21, pp. 32983–32995, 2021.

[15] K. Li, N. M. Y. Zhang, N. Zhang, T. Zhang, G. Liu, and L. Wei, "Spectral characteristics and ultrahigh sensitivities near the dispersion turning point of optical microfiber couplers," *J. Lightw. Technol.*, vol. 36, no. 12, pp. 2409–2415, Jun. 15, 2018.

[16] S. Xu *et al.*, "Ultrasensitive enhanced fabrication-tolerance refractometer based on PANDA-air-hole microfiber at the birefringent dispersion turning point," *Opt. Exp.*, vol. 29, no. 3, pp. 3694–3707, 2021.

[17] G. B. Hocker, "Fiber-optic sensing of pressure and temperature," *Opt. Soc. Amer.*, vol. 18, no. 9, pp. 1445–1448, 1979.

[18] F. Li *et al.*, "Investigation on the response of fused taper couplers to ultrasonic wave," *Appl. Opt.*, vol. 54, no. 23, pp. 6986–6992, 2015.

[19] J.-M. Savolainen, L. Grüner-Nielsen, P. Kristensen, and P. Balling, "Measurement of effective refractive-index differences in a few-mode fiber by axial fiber stretching," *Opt. Exp.*, vol. 20, no. 17, pp. 18646–18651, 2012.

[20] H. P. Luo *et al.*, "Refractive index sensitivity characteristics near the dispersion turning point of the multimode microfiber-based Mach–Zehnder interferomete," *Opt. Lett.*, vol. 40, no. 21, pp. 5042–5045, 2015.

[21] H. Jinqing and H. Bingchen, "Ultrasensitive refractive index sensor based on optical fiber couplers assisted with Vernier effect," *Acta Optica Sinica*, vol. 40, no. 2, 2020, Art. no. 0206002.

[22] C. Yin *et al.*, "Temperature-independent ultrasensitive Fabry–Perot all-fiber strain sensor based on a bubble-expanded microcavity," *IEEE Photon. J.*, vol. 6, no. 4, pp. 1–9, Aug. 2014.

[23] J. Du and Z. He, "Sensitivity enhanced strain and temperature measurements based on FBG and frequency chirp magnification," *Opt. Exp.*, vol. 21, no. 22, p. 27111, Nov. 2013, doi: 10.1364/OE.21.027111.

[24] X. Gao *et al.*, "A dual-parameter fiber sensor based on few-mode fiber and fiber Bragg grating for strain and temperature sensing," *Opt. Commun.*, vol. 454, Jan. 2020, Art. no. 124441.

[25] J. Ruan, "High sensitivity Sagnac interferometric strain sensor based polarization maintaining fibre enhanced coupling," *IET Optoelectron.*, vol. 15, no. 1, pp. 48–51, Feb. 2021.

Jiajie Wen received the bachelor's degree from the Changchun University of Technology, where he is pursuing the master's degree. His main research interests lie in photoelectric signal demodulation and processing.

Xiangyu Yan received the bachelor's degree from the Jinling Institute of Technology. He is currently pursuing the master's degree with Jinan University. His main research content is optical fiber sensor.

Xu Gao received the bachelor's degree from Jilin University (JLU), China, in 2009, and the Ph.D. degree from the Changchun Institute of Optics, Fine Mechanics and Physics (CIOMP), China, in 2014. She is now working with the School of Opto-Electronic Engineering, Changchun University of Science and Technology (CUST). Her current research interests include photoelectric precise displacement measurement technology and photoelectric sensors.

Kaiwei Li (Member, IEEE) received the B.E. degree in mechanical engineering from Jilin University, Changchun, China, in 2009, and the Ph.D. degree in mechanical engineering from the Changchun Institute of Optics, Fine Mechanics and Physics, Chinese Academy of Sciences, Changchun, in 2014. In 2015, he joined the Centre for Optical Fibre Technology, Nanyang Technological University, Singapore, as a Research Fellow. In 2019, he joined the Institute of Photonics Technology, Jinan University, Guangzhou, China. In 2022, he joined the Key Laboratory of Bionic Engineering, Ministry of Education, Jilin University. His research interests include fiber-optic sensors and specialty optical fibers.

Jiajia Wang received the B.E. degree in mechanical engineering and the Ph.D. degree in agricultural mechanization engineering from Jilin University, Changchun, China, in 2009 and 2014, respectively. Then, she joined the College of Agricultural Equipment Engineering, Henan University of Science and Technology, Luoyang, China. Her research interests include optical sensors and their applications in agriculture.